

Calculation of terminal falling velocity of spherical particles moving through polymer solutions using a Power-law viscosity model

Ivan Machač and Bedřich Šiška*

*Institute of Environmental and Chemical Engineering,
The University of Pardubice, CZ–532 10 Pardubice, Czech Republic*

Received: May 31, 2019; Accepted: June 24, 2019

The paper deals with the determination of the terminal velocity of solid spherical particles falling slowly in unbounded purely viscous shear-thinning polymer solutions. The relationships are given for calculation of a sphere terminal velocity falling in the creeping flow region using a power-law viscosity model. The comparison is presented for terminal velocities calculated according to the aforementioned relationships with those obtained experimentally by measuring the terminal velocity of spheres in the aqueous solutions of polymers. By considering the shape of the viscosity function of the polymer solutions, it was necessary to use a simple iterative method to estimate the suitable interval of shear rates for determination of the power-law model parameters.

Keywords: Sphere free fall; Non-Newtonian fluids; Creeping flow; Power-law model

Introduction

A knowledge of the terminal velocity of a rigid particle is necessary for the solution of numerous theoretical and practical problems such as, for example, design calculations of thickeners, fluidised bed equipment, pipeline transport systems, falling particle viscometry, etc. A comprehensive review of literature and an analysis of the investigation of the motion of particles falling freely in a fluid, especially in non-Newtonian one, are given in the book by Chhabra [1].

* Corresponding author, ✉ Bedrich.Siska@upce.cz

Prediction of the terminal falling velocity is based on the knowledge of the drag coefficient c_D of the flow around the particle. For a sphere falling at its terminal velocity u_t , the coefficient c_D is related to the terminal falling velocity u_t by the expression

$$c_D = \frac{4}{3} \frac{gd(\rho_s - \rho)}{\rho u_t^2} \quad (1)$$

Here, g is the gravity acceleration, d the sphere diameter, ρ_s the sphere density, and ρ the liquid density. If the drag coefficient c_D is known, the terminal velocity u_t can simply be calculated from Eq. (1).

For the determination of the drag coefficient in the flow in purely viscous non-Newtonian fluids, different rheological viscosity models are used [1]. In solving engineering problems, a frequently used model is — for its simplicity — the two-parameter power-law (Ostwald-de Waele model)

$$\eta = K\dot{\gamma}^{n-1} \quad (2)$$

where η is the shear viscosity, $\dot{\gamma}$ the shear rate, K the fluid consistency coefficient, and n the power-law index. The disadvantage of this model is that it describes the course of the viscosity dependence on the shear rate with a sufficient accuracy only in the limited intervals (nearly linear in the log-log coordinate system) of the shear rate. Therefore, when calculating the falling velocity u_t of a particle, it is first necessary to estimate the appropriate viscosity function interval in order to determine the values of K and n parameters of the power-law. Beside other, the power-law predicts unreal high values of the apparent viscosity at sufficiently low shear rates.

In this paper, the results are presented of an iterative calculation of terminal velocities of spheres falling in unbounded purely viscous polymer solutions using the power-law. The calculated values of the terminal velocities are compared with those obtained experimentally by Strnadel [2,3].

Fundamentals

Analogously to Newtonian flow, the drag coefficient c_D for the fall of a sphere in an unbounded purely viscous non-Newtonian fluid and for the creeping flow can be expressed as

$$c_D = \frac{24}{Re_n} X_n \quad (3)$$

where

$$Re_n = \frac{\rho u_t^{2-n} d^n}{K} \quad (4)$$

is the power-law Reynolds number and $X_n(n)$ is the drag coefficient corrective factor depending on the power-law index n .

After expressing the coefficient c_D in the equation (1) according to the relation (3), we get for the terminal velocity of a sphere falling in a power-law fluid the relationship

$$u_t = \left[\frac{gd^{1+n}(\rho_s - \rho)}{18KX_n(n)} \right]^{\frac{1}{n}} \quad (5)$$

The functional dependences of X_n on n reported by different investigators differ widely from each other [1]. Nevertheless, the results of the numerical solution of the flow of a power-law fluid around a sphere in the creeping flow region obtained by the authors [2,4–6] coincide very well. The resulting values of the factor X_n are along with their average values $X_{n,av}$ summarized in Table 1. The values of $X_{n,av}$ can be determined with the mean relative deviation of 0.3 % according to the relationship

$$X_n = 0.270 n^3 - 1.666 n^2 + 1.133 n + 1.264 \quad (6)$$

The comparison of the values $X_{n,av}$ with those calculated according to Eq. (6) is shown in Fig. 1.

Table 1 Computed values of the drag coefficient corrective factor X_n

n	Strnadel and Machač [2]	Crochet et al. [4]	Gu and Tanner [5]	Tripathi et al. [6]	Average value $X_{n,av}$
1	1.000	1.020	1.002	1.003	1.006
0.9	1.137	1.180	1.140	1.141	1.149
0.8	1.258	1.270	1.24	1.230	1.249
0.7	1.355	1.350	1.320	1.316	1.335
0.6	1.429	1.440	1.382	1.381	1.408
0.5	1.476	1.470	1.420	1.420	1.447
0.4	1.495	1.510	1.442	1.440	1.472
0.3	1.484	1.480	1.458	1.460	1.471
0.2	1.436	1.460	1.413	1.398	1.427
0.1	1.341	1.390	1.354	1.360	1.361

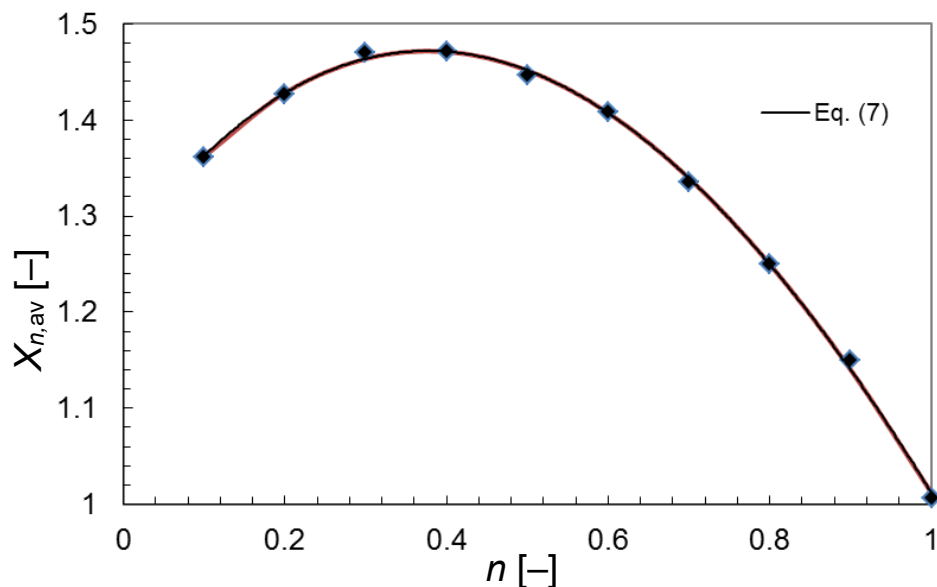


Fig. 1 Dependence of the corrective drag coefficient factor $X_{n,av}$ on the flow index n

Materials and methods

The relevant falling sphere experiments were carried out in six types of cylindrical Perspex columns filled with aqueous solutions of Carboxymethyl Cellulose (CMC), Hydroxyethyl Cellulose Natrosol, and Methyl Ethyl Cellulose Tylose. The diameters of the columns were 16, 21, 26, 34, 40, and 90 mm which led to the ratio $d/D \in (0.011; 0.499)$. The polymer solutions were prepared by dissolution of powdered polymers in demineralised water. The composition of test liquids along with their density is summarized in Table 2. The measurements of liquid flow curves, primary normal stress differences, oscillatory, creep & recovery, stress relaxation and stress growth tests were carried out in a rheometer Haake MARS II (Thermo Fisher Scientific, Karlsruhe, Germany).

Table 2 Characteristics of the liquids tested

Liquid	Polymer Used	Concentration [wt. %]	Density [kg m^{-3}]
L1	Methyl Ethyl Cellulose Tylose	3.0	1006
L2	Carboxymethyl Cellulose	1.2	1002
L3	Hydroxyethyl Cellulose Natrosol 250 HHX)	1.0	1000

Seventeen types of spherical particles made of glass, ceramics, steel, lead, and tungsten carbide were used for the drop tests. Typical characteristics of the individual test particles are given in Table 3.

Table 3 Specifications of the spherical particles tested

Particle	Material	d [mm]	ρ_s [kg m ⁻³]	Particle	Material	d [mm]	ρ_s [kg m ⁻³]
S1	glass	1.93	2525	S10	ceramics	7.99	3908
S2	glass	3.13	2486	S11	carbide	0.99	15119
S3	glass	4.12	2597	S12	carbide	1.49	15119
S4	glass	4.93	2508	S13	carbide	1.99	15119
S5	glass	6.12	2495	S14	carbide	2.99	15119
S6	ceramics	1.99	3908	S15	steel	0.99	7526
S7	ceramics	2.99	3908	S16	steel	3.17	7789
S8	ceramics	3.99	3908	S17	lead	2.00	11118
S9	ceramics	5.99	3908	–	–	–	–

The values of the terminal falling velocities $u_{t,\text{exp}}$ in unbounded fluid were determined by a linear extrapolation of the experimental dependences of the terminal falling velocities measured in the individual test columns on the ratio d/D to the value $d/D \rightarrow 0$. The terminal falling velocities $u_{b,\text{exp}}$ obtained had ranged in the intervals 0.43–11.4 mm s⁻¹ for the Tylose solution, 0.57–38.0 mm s⁻¹ for the CMC solution, and 0.77–49.7 mm s⁻¹. This corresponded to the Reynolds number Re_n varying from 1.19×10^{-4} to 0.153. The achieved effective shear rate $\dot{\gamma}_{\text{ef}}$ estimated by the ratio $u_{b,\text{exp}}/d$ ranged from 0.22 s⁻¹ to 3.8 s⁻¹ for the Tylose solution, from 0.30 s⁻¹ to 13 s⁻¹ for the CMC solution, and from 0.70 s⁻¹ to 16 s⁻¹ for the Natrosol solution.

All experiments are described in more detail elsewhere (see [2,3]).

Results and discussion

Rheological measurements

The viscosity functions of the test polymer solutions, evaluated from the experimentally obtained flow curves, are displayed in Fig. 2. It is evident that the course of these functions can be approximated by the power-law model (2) only in the narrow intervals of shear rates (Table 4).

It followed from the creep & recovery tests and normal stress measurements [2,3] that the test polymer solutions exhibit a negligible elastic behaviour and can thus be considered as purely viscous (inelastic) liquids.

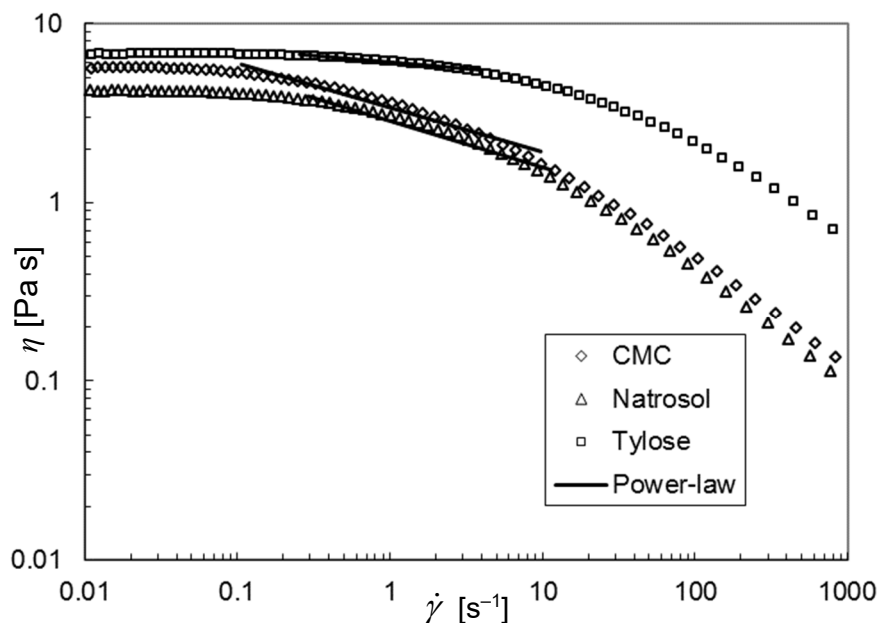


Fig. 2 Viscosity functions of the model polymer solutions

Table 4 Shear rate intervals and power-law parameters of the liquids tested

Liquid	$\Delta\dot{\gamma}_g$ [s ⁻¹]	n [-]	K [Pa s ⁿ]	$\delta_{m,pl}$ [%]	$\delta_{max,pl}$ [%]	$\Delta\dot{\gamma}_c$ [s ⁻¹]	δ_m [%]	δ_{max} [%]
L1	0.07–1.0	0.964	6.34	–	–	0.22–3.6	5.1	10.9
	0.26–3.9	0.927	6.08	1.0	2.7	0.21–3.8	4.4	10.5
L2	0.10–1.1	0.842	3.76	–	–	0.29–6.9	14.8	45.9
	0.29–6.2	0.731	3.54	–	–	0.16–9.7	13.4	30.0
L3	0.10–9.7	0.753	3.39	5.5	17.0	0.26–9.0	7.6	29.0
	0.07–1.2	0.884	3.134	–	–	0.40–8.1	16.7	51.4
	0.4–7.7	0.739	2.972	–	–	0.31–10.8	16.5	34.8
	0.29–11.4	0.742	2.852	4.4	11.8	0.32–11.7	9.7	29.9

The courses of the creep & recovery tests are shown in Fig. 3. The primary normal stress differences of the solutions were at the relevant shear rates due to their small and unmeasurable values.

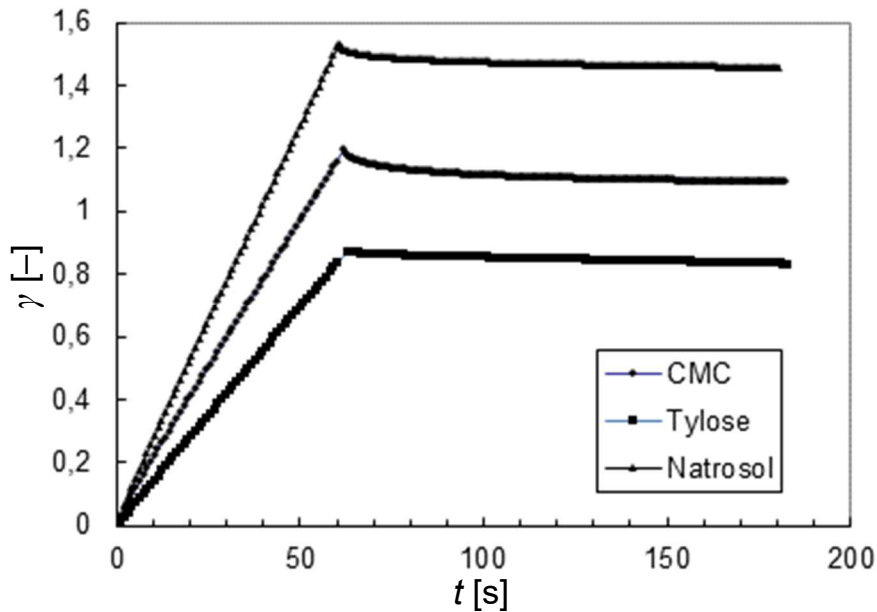


Fig. 3 Creep & recovery tests of the model polymer solutions

Terminal falling velocity

Before calculating the terminal velocity $u_{t,c}$ of spheres characterized in Table 3 according to the relationships (5) and (6), the parameters K and n of the power-law (2) were determined from the course of the liquid viscosity functions in an initial guess $\Delta\dot{\gamma}_g$ of the shear rate interval. Then, using the calculated values $u_{t,c}$, the suitability of the selected shear rate interval was verified by calculating the effective shear rates $u_{t,c}/d$. If the calculated values $u_{t,c}/d$ do not correspond with the shear rate interval $\Delta\dot{\gamma}_g$, the shear rate guess must be corrected and the determination of K and n parameters and the calculation of the terminal velocities $u_{t,c}$ repeated.

The guesses $\Delta\dot{\gamma}_g$, corresponding values of the parameters K and n , and subsequently calculated values $\Delta\dot{\gamma}_c$ are for individual test liquids given in Table 4. This table also shows the mean relative deviations δ_m and maximum relative deviations δ_{max} of the calculated and experimental values of the terminal falling velocities. It is evident that the gradual change of the interval $\Delta\dot{\gamma}_g$ leads to the accordance between intervals $\Delta\dot{\gamma}_g$ and $\Delta\dot{\gamma}_c$ and the deviations δ_m and δ_{max} decrease.

The best agreement of the $u_{t,c}$ and $u_{t,exp}$ values was achieved for the Tylose solution. In this case, the power-law approximates the relevant part of the viscosity function with the mean relative deviation of experimental and calculated viscosity data $\delta_{m,pl} = 1.0\%$. At the same time, the effective shear rates $u_{t,c}/d$ are low and the shear-thinning of the solution not very significant ($n = 0.927$). A worse

agreement of the calculated and experimental data of terminal velocities was achieved in the case of the fall of particles in the CMC and Natrosol solutions. Herein, the relevant parts of the viscosity function are approximated by the power-law with the larger errors δ_{pl} (see Table 4). Moreover, considering that at lower shear rates the power-law predicts a higher liquid viscosity than its real value, there is an overestimation of the frictional resistance and the calculated terminal velocities are lower than those obtained experimentally. Simultaneously, the deviations δ_m increase with the increasing shear rates. These facts are evident from Fig. 4, in which the terminal velocities $u_{t,c}$ and $u_{t,exp}$ are compared for CMC and Natrosol solutions.

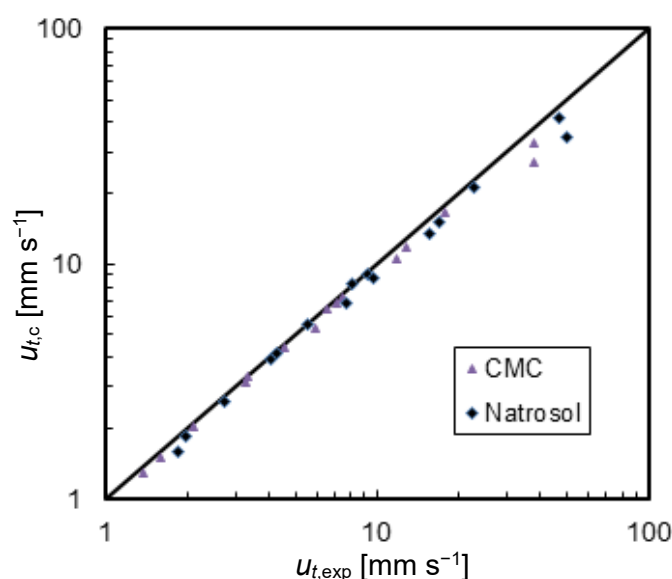


Fig. 4 Comparison of the terminal velocities $u_{t,c}$ and $u_{t,exp}$ for CMC and Natrosol solutions

Higher accuracy of approximation of the viscosity function by power-law for CMC and Natrosol solutions can be achieved by dividing the relevant shear rate interval into two sub-intervals. For the solution of CMC, the power-law parameters $K = 3.54 \text{ Pa s}^n$ and $n = 0.797$ ($\delta_{m,pl} = 3.0 \%$, $\delta_{max,pl} = 9.4 \%$) were determined in the shear rate interval from 0.1 to 3.2 s^{-1} and $K = 4.15 \text{ Pa s}^n$ and $n = 0.602$ ($\delta_{m,pl} = 1.2 \%$, $\delta_{max,pl} = 3.1 \%$) in the interval from 3.0 to 9.7 s^{-1} . After recalculation of the terminal velocity of particles, it was found that the deviations of the calculated and experimental values decreased only in the interval of lower values of the shear rate (particles S1–S9, S11, S15, S17, $\delta_m = 4.4 \%$, $\delta_{max} = 11.1 \%$). On the contrary, in the interval of higher shear rates, due to worse prediction of the polymer solution viscosity at lower shear rates by power-law, a higher deviation of calculated and experimental values of terminal velocities were found ($\delta_m = 22.2 \%$, $\delta_{max} = 27.2 \%$). Analogous results were obtained for the calculation of terminal velocity of particles in the Natrosol solution. Here, the power-law

parameters $K = 2.92 \text{ Pa s}^n$ and $n = 0.815$ ($\delta_{m,pl} = 2.9 \%$, $\delta_{max,pl} = 5.6 \%$) were determined in the shear rate interval from 0.3 to 3.2 s^{-1} and $K = 3.67 \text{ Pa s}^n$ and $n = 0.594$ ($\delta_{m,pl} = 1.2 \%$, $\delta_{max,pl} = 2.51 \%$) in the interval from 3.0 to 9.7 s^{-1} .

Also in this case, it was found that the deviations of the recalculated and experimental values of terminal velocity decreased only in the interval of lower values of the shear rate (particles S1–S8, S11, S15, $\delta_m = 4.8 \%$, $\delta_{max} = 10.1 \%$). In the interval of higher shear rates the deviations of calculated and experimental values of terminal velocities were $\delta_m = 19.5 \%$ and $\delta_{max} = 21.1 \%$.

Conclusions

The relationships for calculating the terminal velocity of spherical particles falling slowly in an unbounded power-law fluid have been presented including a new simple formula for determination of the drag coefficient corrective factor. Simultaneously, a simple iterative procedure has been proposed for calculation of the terminal velocity of spheres falling in purely viscous polymer solutions whose viscosity function can be approximated by the power-law only in the limited range of shear rate.

Applicability of this procedure has been verified comparing the calculated values of terminal velocity of spheres falling in the Tylose, CMC, and Natrosol polymer solutions with the experimental data. A very good agreement between calculated and experimental terminal velocity data has been achieved in the domain of low values of the effective shear rates u_t/d . Here, the shear-thinning of the liquid is moderate and for the flow index of the approximated part of the viscosity function it is approximately valid that $n > 0.8$. At higher shear rates, the degree of shear-thinning of the polymer solution tested increases, the flow index n of the approximated part of the viscosity function decreases, which leads to a more pronounced underestimation of the calculated values of the particle terminal velocity. Greater accuracy of the terminal velocity prediction in this case is achieved, for example, by using relationships that are based on the Carreau viscosity model, which includes the zero shear-rate viscosity η_0 as a specific parameter [1,3].

Symbols

c_D	drag coefficient	–
d	sphere diameter	m
D	diameter of test column	m
G	gravity acceleration	m s^{-2}
K	power-law parameter (consistency coefficient)	Pa s^n
n	power-law parameter (flow index)	–

Re_n	power-law Reynolds number	–
u_t	particle terminal falling velocity	m s^{-1}
$u_{t\infty}$	particle terminal falling velocity in unbounded liquid	m s^{-1}
X_n	drag coefficient corrective factor	–

Greek symbols

γ	deformation	–
$\dot{\gamma}$	shear rate	s^{-1}
δ	relative deviation	%
η	non-Newtonian (apparent) shear viscosity	Pa s
η_0	zero shear-rate viscosity	Pa s
ρ	fluid density	kg m^{-3}
ρ_s	particle density	kg m^{-3}

Subscripts

c	calculated value
ef	effective value
exp	experimental value
g	guess value
m	mean value
max	maximum value
pl	related to power-law

References

- [1] Chhabra R.P.: *Bubbles, Drops, and Particles in Non-Newtonian Fluids*, 2nd Ed. CRC Press, Boca Raton 2006.
- [2] Strnadel J.: *Fall of a rigid single spherical particle in non-Newtonian fluids* (in Czech), Ph.D. Thesis, University of Pardubice, Pardubice 2011.
- [3] Strnadel J., Simon M., Macháč I.: Wall effects on terminal falling velocity of spherical particles moving in a Carreau model fluid. *Chemical Papers* **65** (2011) 177–184.
- [4] Crochet M.J., Davies A. R., Walters K.: The Flow of a Power-Law Fluid Around a Sphere, in: *Numerical simulation of non-Newtonian flow*, Rheology series 1. Elsevier, New York 1984; pp. 252–257.
- [5] Gu D., Tanner R.I.: The drag on a sphere in a power-law fluid. *Journal of Non-Newtonian Fluid Mechanics* **17** (1985) 1–12.
- [6] Tripathi A., Chhabra R.P., Sundarajan T.: Power-law fluid flow over spheroidal particles. *Industrial & Engineering Chemistry Research* **33** (1994) 403–410.